Author Manuscript

Author Manuscript

Author Manuscript

Author Manuscript

HHS Public Access

Author manuscript

Neurorehabil Neural Repair. Author manuscript; available in PMC 2025 August 16.

Published in final edited form as:

Neurorehabil Neural Repair. 2025 September ; 39(9): 715–727. doi:10.1177/15459683251340914.

Loss of joint individuation and abnormal synergy post stroke in upper limb movements

Kyung Koh[1,2], **Giovanni Oppizzi**[1,2], **Raziyeh Baghi**[2], **Glenn Kehs**[3,4], **Li-Qun Zhang**[1,2,5]

[1]Fischell Department of Bioengineering, University of Maryland, College Park, MD 20742

[2]Department of Physical Therapy & Rehabilitation Science, University of Maryland, Baltimore, MD 21201

[3]University of Maryland Rehabilitation and Orthopaedic Institute, Baltimore, MD

[4]Department of Neurology, University of Maryland, Baltimore, MD 21201

[5]Department of Orthopaedics, University of Maryland, Baltimore, MD 21201

Abstract

Stroke often leads to long-term impairments in upper extremity (UE) motor function, including muscle weakness, spasticity, and abnormal joint synergies, which hinder independent joint control and daily activities. This study examined multi-joint motor impairments and characterized abnormal synergy patterns post-stroke using a robotic exoskeleton. The exoskeleton independently controlled shoulder, elbow, and wrist joints while measuring responses across all joints during horizontal plane movements. Fifty-three stroke survivors and 24 age-matched controls performed single-joint movements under constrained (fixed joints) and unconstrained (free joints) conditions. Coupled range of torques (ROT) and range of motion (ROM) at non-instructed joints were calculated relative to instructed joint movements and summarized in a 3x3 matrix. Stroke survivors showed significantly higher coupling torques and motions at non-instructed joints compared to controls, with the greatest impairments in isolating distal movements, particularly in a proximal-to-distal gradient. Abnormal synergy patterns were systematically identified, revealing that stroke survivors exhibited two common patterns for shoulder and elbow tasks, marked by excessive coupling at neighboring joints. For wrist movement tasks, four distinct patterns emerged, involving excessive coupling at both shoulder and elbow joints. These findings demonstrate characteristic impairments in joint individuation and synergy following a stroke, providing a framework to understand motor deficits and guide rehabilitation strategies aimed at restoring joint-specific control.

Keywords

stroke; upper extremity; motor impairment; joint individuation; synergy patterns; rehabilitation

Correspondence to: Li-Qun Zhang, PhD, Department of Physical Therapy & Rehabilitation Science, Department of Orthopaedics, University of Maryland, Baltimore, 100 Penn St, Baltimore, MD 21201, l-zhang@som.umaryland.edu.

Competing interests

The authors declared no potential conflicts of interest with respect to the research, authorship, and/or publication of this article.

Author Manuscript Author Manuscript Author Manuscript Author Manuscript

Introduction

About 795,000 people suffer strokes every year in the United States and stroke is the third leading cause of death[1]. Almost three quarters of all strokes occur in people over the age of 65 and with an ever-increasing elderly population, stroke will continue to be a major health issue[1]. Motor impairment in the upper extremity (UE) is a prevalent deficit following stroke, with approximately two-thirds of stroke survivors experiencing long-term reductions in UE motor function. This impairment, often manifesting as abnormal synergy patterns, severely limits the ability to perform daily activities, reduces productivity, and hampers social engagement, underscoring the need for detailed analysis of synergy patterns to inform rehabilitation strategies[2–5].

UE motor impairments in individuals post stroke may be attributed in part to a loss of individuation (LOI). The LOI is an inability to voluntarily move a joint independently of the other joints. Traditionally, the LOI has been described as abnormal synergy that are often observed in stroke survivors[6]. Previous quantitative studies described the LOI as disturbed limb dynamics[7] and disrupted inter-joint coordination[8] during reaching movements. However, few studies have directly investigated how LOI is related to stroke. Most studies have exclusively focused on finger movements,[9,10] and to our knowledge, only one study explored LOI in the UE by assessing non-instructed joints (i.e. angular movement) during single-joint tasks[11]. Nevertheless, this study did not systematically investigate coordination deficits in terms of both kinematics and kinetics. Given that the understanding of UE coordination deficits in stroke survivors is critical for better identification of motor impairment and planning for rehabilitation,[12–14] a more comprehensive investigation of LOI that encompasses all aspects of kinematics and kinetics is required to further elucidate the mechanisms of motor deficits post-stroke and to develop more targeted rehabilitation approaches[15].

Clinical scales including Fugl-Meyer Motor Assessment (FMA) [11], modified Ashworth scale (MAS), and Chedoke McMaster Stroke Assessment (CMA) are used to evaluate impairments and functional limitations related to LOI in individuals with stroke. However, it is not feasible for a clinician to quantitatively assess LOI with these scales, as they lack the resolution to capture subtle deficits in joint individuation and abnormal synergy patterns across multiple joints. To address this clinical gap, robotic technologies such as the IntelliArm provide precise, objective measurements of multi-joint motor impairments that traditional assessments cannot capture [6,12,13]. Using a divide-and-conquer approach, the IntelliArm is capable of controlling an individual joint (one joint at a time) and simultaneously measuring shoulder, elbow, and wrist joint excursions, allowing for comprehensive quantification of both kinematic and kinetic aspects of LOI. This capability enables systematic characterization of multi-joint coordination deficits and abnormal synergy patterns, which are critical for developing targeted rehabilitation strategies.

Abnormal synergies and loss of individuation post-stroke are believed to arise from both neural and biomechanical factors, including damage to the corticospinal tract (CST) and compensatory recruitment of alternative descending pathways, such as the reticulospinal tract (RST) [1]. The CST predominantly controls fine motor movements, especially in distal

Author Manuscript Author Manuscript Author Manuscript Author Manuscript

muscles, while the RST influences proximal and axial muscles [2]. Damage to the CST can lead to impaired fine motor control, and the subsequent upregulation of the RST may result in generalized activation of muscle groups, leading to involuntary coupling of joint movements [3]. This neural reorganization provides a theoretical basis for the proximal-to-distal gradient of impairments, where distal joints, relying heavily on CST input, experience more severe deficits compared to proximal joints [4]. However, some studies have reported an absence of a proximal-to-distal gradient in motor deficits early after stroke, suggesting that loss of hand function may be due to an inability to move multiple segments of the upper extremity, not just the distal ones [5]. These findings highlight the complexity of motor impairments post-stroke and underscore the need for comprehensive assessments of both proximal and distal joint functions [6].

Here, we systematically investigated LOI in the UE post stroke in aspects of kinetics and kinematics and its correlations with functional impairments measured by clinical scales. A custom multi-joint rehabilitation robot called IntelliArm, developed previously for quantitative and systematic characterizations of UE neuromechanical changes post stroke,[17] was used to control and measure joint excursion at the shoulder, elbow and wrist joints individually and simultaneously. We presented a novel approach to identify LOI in different aspects by allowing to quantify 9 coupling patterns of UE movements. In individual joint control, distal joint and proximal joints may have different degrees of impairment post stroke. In previous studies of robot-aided rehabilitation of UE post stroke, it was found that distal joint (wrist or finger) training leads to additional motor improvements in the proximal joints, while the proximal joints (i.e., the elbow and shoulder joints) were restricted to move in the training[25–27]. The improvement on proximal joints may be attributed to the enhanced ability to control individual joints. Thus, we hypothesized that LOIs would be more severe from the proximal to distal joints.

Materials and methods

Participants

Fifty-three stroke survivors (34 males and 19 females, mean age 58 years, SD 13.1) and 24 age-matched control subjects without any neurological disorder (13 males and 11 females, mean age 49.2 years, SD 15.8) were recruited for this study. Demographic data for stroke survivors are shown in Table 1. All the control subjects were right-handed. Inclusion criteria of the stroke survivors were 1) first focal unilateral lesion, ischemic or hemorrhagic; 2) had cognitive ability to follow simple instructions; 3) ability to provide informed consent. Individuals were excluded if they had: 1) apraxia; 2) severe cardiovascular conditions; 3) unrelated UE musculoskeletal injuries. Prior to the experiment, each participant gave an informed consent approved by the institutional review board.

Experimental procedures

To assess upper extremity (UE) impairment, we used the IntelliArm rehabilitation robot, designed for reaching motions in the horizontal plane with gravity-supported UE movement (Fig. 1a). Subjects sat upright comfortably with their upper arm, forearm, and hand secured to the IntelliArm braces (Fig. 1). The robot arm lengths were adjusted to align its mechanical

Author Manuscript Author Manuscript Author Manuscript Author Manuscript

axes with the shoulder horizontal adduction/abduction and elbow and wrist flexion/extension axes. Proper alignment was verified through visual inspection and joint motion testing. Straps ensured alignment throughout the experiment. The initial position was set at shoulder horizontal adduction of 70°, elbow flexion of 60°, and wrist flexion of 0° with the forearm in a neutral (mid-pronation/supination) position to standardize wrist orientation across subjects (Fig. 1b). A novel robust impedance control made the IntelliArm backdrivable by minimizing inertia and damping, allowing free movement of the shoulder, elbow, and wrist while eliminating the influence of gravity.

Subjects performed five cycles of back-and-forth flexion-extension (horizontal adduction-abduction for shoulder) movements at the selected intended joint while minimizing non-instructed joint motion. Movement speed was self-selected based on each subject's preferred movement speed to ensure comfort and natural performance. The robot joint for the instructed joint was set to a backdrivable mode, allowing free movement. Movements were performed one joint at a time (shoulder, elbow, or wrist), with systematic repetition across all joints[28]. Tasks were conducted under two conditions: constrained, where non-instructed joints were restricted by the IntelliArm, and unconstrained, where all joints were backdrivable. Joint torque and angular movement were recorded simultaneously. Post-stroke LOI was quantitatively assessed by analyzing coupled torque and angular movement at non-instructed joints, normalized to the instructed joint's range of motion to standardize unintended movement measurements[28].

Clinical evaluations assessed upper limb motor function and spasticity in study participants. Upper limb motor function was evaluated using the Fugl-Meyer Assessment of the upper limb (FMA-UE) and the Action Research Arm Test (ARAT). FMA-UE, a reliable tool with a maximum score of 66, measures motor function and includes separate components for proximal (maximum score of 42) and distal (maximum score of 24) functions[29,30]. This division allows for a detailed assessment of motor recovery, as recovery from hemiplegia often progresses from proximal to distal muscles. ARAT, with a maximum score of 57, evaluates functional tasks such as grasp, grip, pinch, and gross movement[31]. Spasticity in both the elbow flexors/extensors and wrist flexors/extensors using the Modified Ashworth Scale (MAS), which grades spasticity from 0 (no increase in muscle tone) to 4 (rigid in flexion and extension)[32,33].

Data analysis

The start and end of movement in each trial were defined as the points when the instructed joint reached its maximum and minimum angles during cyclic movement. Maximum angles represent full flexion (wrist and elbow) or full horizontal adduction (shoulder), while minimum angles represent full extension or full horizontal abduction. Movements started from the initial position described in the experimental procedures, with subjects performing cyclic motions around this point. In this study, inward movements refer to motions directed toward the body (minimum to maximum angles: full extension/abduction to full flexion/adduction), whereas outward movements refer to motions directed away from the body (maximum to minimum angles: full flexion/adduction to full extension/abduction). The direction of inward and outward movements for each joint is depicted in Figure 1b.

Author Manuscript Author Manuscript Author Manuscript Author Manuscript

Instructed joint performance was evaluated by movement rate, smoothness, range of motion (ROM), and range of torque (ROT)[28]. Movement smoothness was quantified using spectral arc length (SPARC), which measures the Fourier magnitude spectrum's arc length within an adaptive frequency range[34]. SPARC identifies movement intermittencies independently of amplitude or duration, making it suitable for detecting deficits despite ROM and movement rate differences between stroke and control groups. Due to data length limitations, SPARC was analyzed only for whole movement. The calculation was as follows:

$$SPARC = -\int_0^{\omega_c} \left[\left(\frac{1}{\omega_c}\right)^2 + \left(\frac{d\hat{A}(\omega)}{d\omega}\right)^2\right]^{\frac{1}{2}} d\omega \tag{1}$$

$$\hat{A}(\omega) = \frac{A(\omega)}{A(0)} \tag{2}$$

$$\omega_c \triangleq min\left\{\omega_c^{max}, min\left\{\omega \mid \hat{A}(r) < \overline{A}, \forall r > \omega\right\}\right\} \tag{3}$$

where $A(\omega)$ is the Fourier magnitude spectrum of the velocity signal v(t), $\hat{A}(\omega)$ is the normalized magnitude spectrum.

The kinematic LOI matrix (X_θ) and kinetic LOI matrix (X_τ) were used to quantify the relative movement of non-instructed joints with respect to the instructed joint. This analysis method, which has been well-established in previous studies for evaluating inter-joint coordination, enables consistent comparisons of joint coupling by using the instructed joint as a reference[28,35]. Matrix elements represent coupling ratios, with X_τ defining torque coupling and X_θ defining angle coupling.

$$X_\tau = \begin{bmatrix} X_{\tau 11} & X_{\tau 12} & X_{\tau 13} \\ X_{\tau 21} & X_{\tau 22} & X_{\tau 23} \\ X_{\tau 31} & X_{\tau 32} & X_{\tau 33} \end{bmatrix} = \begin{bmatrix} \tau_{11}/\theta_{11} & \tau_{12}/\theta_{11} & \tau_{13}/\theta_{11} \\ \tau_{21}/\theta_{22} & \tau_{22}/\theta_{22} & \tau_{23}/\theta_{22} \\ \tau_{31}/\theta_{33} & \tau_{32}/\theta_{33} & \tau_{33}/\theta_{33} \end{bmatrix} \tag{4}$$

$$X_\theta = \begin{bmatrix} \theta_{11}/\theta_{11} & \theta_{12}/\theta_{11} & \theta_{13}/\theta_{11} \\ \theta_{21}/\theta_{22} & \theta_{22}/\theta_{22} & \theta_{23}/\theta_{22} \\ \theta_{31}/\theta_{33} & \theta_{32}/\theta_{33} & \theta_{33}/\theta_{33} \end{bmatrix} = \begin{bmatrix} 1 & \theta_{12}/\theta_{11} & \theta_{13}/\theta_{11} \\ \theta_{21}/\theta_{22} & 1 & \theta_{23}/\theta_{22} \\ \theta_{31}/\theta_{33} & \theta_{32}/\theta_{33} & 1 \end{bmatrix} \tag{5}$$

Author Manuscript Author Manuscript Author Manuscript Author Manuscript

During isolated instructed joint movements, LOI was evaluated using the ratios of coupled torques at non-instructed joints relative to the instructed joint excursion. Using the instructed joint as a reference ensured consistency across trials, despite variations in pre-stroke joint excursion or torque. For example, during selective shoulder horizontal abduction, the ratio $X_{\tau 12} = \tau_{12}/\theta_{11}$, quantified LOI by comparing coupled elbow torque to voluntary shoulder abduction.

Similarly, LOI was evaluated using the ratios of coupled rotations at non-instructed joints relative to instructed joint excursion, defining the angle coupling matrix X_θ. X_τ and X_θ were quantified under both constrained and unconstrained conditions during inward, outward, and whole movements, averaged across five trials. Differences in X_τ or X_θ elements between stroke and control groups were assessed using a relative change ratio, calculated by dividing each stroke group element by the corresponding control group average. In this study, the term ‘abnormal synergies’ specifically refers to unintended inter-joint coupling as measured by LOI. Higher LOI values indicate stronger abnormal coupling between joints, providing an objective metric for quantifying abnormal synergy patterns post-stroke.

Matrix Asymmetry (Joint Proximal-Distal Asymmetry) Measures

To quantify asymmetry in joint coupling during instructed movements, we decomposed the torque coupling matrix X_τ and similarly the angle coupling matrix X_θ into symmetric and anti-symmetric components. The X_τ matrix describes coupled torques at non-instructed joints during instructed joint movement, with the decomposition capturing coordination differences between proximal and distal joints in stroke survivors and controls. This analysis evaluates whether the relative movement of non-instructed joints, measured with respect to the instructed joint, is similar between joint pairs. For example, in the relationship between the shoulder and wrist, symmetry is observed if the wrist’s movement during shoulder instruction is comparable to the shoulder’s movement during wrist instruction. Asymmetry occurs when these relative couplings differ, indicating an imbalance in joint interactions that is independent of movement direction.

The symmetric component of the ($X_{\tau s}$) matrix represents the portion of the joint coupling that is shared symmetrically between the proximal and distal joints, while the anti-symmetric ($X_{\tau a}$) component captures the asymmetric joint coupling. This decomposition allows for the separation of symmetrical coupling (represented by symmetry) from asymmetric coupling (captured by asymmetry). The symmetric part of the matrix was calculated as:

$$X_{\tau s} = \frac{X_\tau + X_\tau^T}{2} \tag{6}$$

The anti-symmetric part was derived as:

$$X_{\tau a} = \frac{X_\tau - X_\tau^T}{2} \tag{7}$$

Author Manuscript Author Manuscript Author Manuscript Author Manuscript

The asymmetry measure was then defined as the ratio of the Frobenius norm of the anti-symmetric part to the symmetric part for the X_τ matrix as follows:

$$\frac{\|X_{\tau a}\|}{\|X_{\tau s}\|} \tag{8}$$

The Frobenius norm $\|\cdot\|$ was used as it provides a matrix-wide measure of magnitude, capturing the overall asymmetry of coupling between joints. By comparing the norms of the anti-symmetric and symmetric components, we obtained a single ratio that represents the extent of asymmetry in the matrix. A higher asymmetry measure indicates greater asymmetry, which reflects increased asymmetric coupling between the proximal and distal joints.

The asymmetry measure provides an objective quantification of abnormal joint coupling, which is critical for understanding motor impairments post-stroke. Higher asymmetry values indicate disproportionate coupling between joints, reflecting impaired ability to independently control individual joints. Clinically, this measure can be used to assess the severity of abnormal synergies, monitor rehabilitation progress, and inform targeted interventions aimed at improving multi-joint coordination. By capturing differences in proximal-distal joint interactions, the asymmetry measure provides valuable insight into motor control deficits that may not be evident through traditional clinical assessments.

Quantification of abnormal coupling patters

To assess simultaneous movement of non-instructed joints during instructed joint movements, we calculated an LOI index,[9,11] defined as the ratio of non-instructed to instructed joint excursion. An LOI near zero indicates good individuation, while higher values reflect greater abnormal coupling.

We used a novel approach to identify nine coordination patterns based on vector coding. For example, during shoulder movement, the LOI at the elbow was plotted against the LOI at the wrist (Fig. 3). These patterns reflect the direction and magnitude of joint coupling. The nine identified patterns are as follows: (1) Normal, characterized by minimal non-instructed joint movement with LOI values near zero; (2) Elbow extension-excursion (EE), indicating unintended elbow extension during instructed movements; (3) Elbow & wrist EE, reflecting simultaneous unintended extension at both the elbow and wrist; (4) Wrist EE, showing unintended wrist extension during other joint movements; (5) Elbow flexion-excursion (FE) & wrist EE, indicating elbow flexion with concurrent wrist extension; (6) Elbow FE, representing unintended elbow flexion; (7) Elbow & wrist FE, reflecting simultaneous unintended flexion at both joints; (8) Wrist FE, indicating unintended wrist flexion; and (9) Elbow EE & wrist FE, showing elbow extension with concurrent wrist flexion. Patterns were categorized into 45° bins to accommodate variability in LOI vectors, as perfect alignment with diagonal or axial directions was rare. In-phase patterns (45° and 225°) represent joints moving in the same direction, whereas anti-phase patterns (135° and 315°) indicate opposing joint motions.

Author Manuscript Author Manuscript Author Manuscript Author Manuscript

Statistical analysis

A three-way repeated measures ANOVA was conducted with factors of Group (Control, Stroke), Direction (inward, outward), and instructed Joint (shoulder, elbow, wrist) to analyze differences in movement rate, smoothness, ROM, and ROT. A four-way repeated measures ANOVA, including non-instructed Joint as a factor, was used to assess X_τ and X_θ. Post-hoc pairwise comparisons with Bonferroni corrections tested group differences, with statistical significance set at p=0.05p = 0.05p=0.05.

One-way ANOVA tested differences among ratios in the X_τ and X_θ matric. Spearman correlation coefficients evaluated relationships between LOI, MAS, and FMA.

Results

Loss of individuation

The X_τ and X_θ matrices characterized LOI in terms of kinetic and kinematic coupling, respectively (Fig. 2). In the unconstrained condition (Fig. 2a), stroke participants exhibited difficulty in individuated joint movements, generating greater coupling at proximal joints when distal joints were instructed. The lower-left off-diagonal elements of X_θ in the stroke group were significantly higher than in controls, confirmed by a repeated measures ANOVA ($F_{2,138}$=3.232, P=0.043) and post-hoc comparisons, showing elevated X_θ at the shoulder during elbow movements (P=0.028) and at both the shoulder (P=0.03) and elbow (P<0.01 during wrist movements. No significant effect was observed for inward versus outward movements.

In the constrained condition (Fig. 2b), a significant interaction was found for Group × Instructed joint × Non-instructed joint ($F_{2,138}$=3.473, P=0.034). Post-hoc analysis revealed higher lower-left off-diagonal X_τ elements in the stroke group, consistent with X_θ. Stroke participants exhibited significantly higher coupling torque at the shoulder during elbow movements (P=0.047) and at both the shoulder (P=0.009) and elbow (P=0.001) during wrist movements. Furthermore, greater wrist coupling torque during shoulder movements (P=0.019), indicating X_τ matrix obtained under isometric conditions is more sensitive in detecting abnormal inter-joint coupling than the X_θ matrix. There was no significant effect on the inward-outward directions.

Asymmetry in the X_τ matrix of stroke survivors showed significantly higher bottom-left off-diagonal elements compared to upper-right elements (P<0.05) , with 1) $X_{\tau 21}$ (7.16 ± 1.38 Nm/rad) greater than $X_{\tau 12}$ (2.79 ± 0.23 Nm/rad) (P<0.05) 2) $X_{\tau 31}$ (6.83 ± 1.47 Nm/rad) greater than $X_{\tau 13}$ (0.54 ± 0.05 Nm/rad) (P<0.01) and 3) $X_{\tau 32}$ (6.70 ± 1.15 Nm/rad) greater than $X_{\tau 23}$ (0.79 ± 0.12 Nm/rad) (P<0.01) (Fig. 2b). Control participants showed no significant difference between $X_{\tau 21}$ (3.02 ± 0.39 Nm/rad) and $X_{\tau 12}$ (2.36 ± 0.34 Nm/rad) (P>0.05), but higher $X_{\tau 31}$ (1.04 ± 0.14 Nm/rad) and $X_{\tau 32}$ (1.01 ± 0.11 Nm/rad) compared to their counterparts (P<0.01). These findings suggest stronger proximal coupling during distal movements in the stroke group.

Author Manuscript Author Manuscript Author Manuscript Author Manuscript

The stroke group's X_τ symmetry measure ($\|X_{\tau a}\|/\|X_{\tau s}\|$) indicated significantly greater asymmetry than the control group ($P<0.01$), indicating intended distal joint movement had significantly higher coupling effect at the proximal joints than the coupling in the opposite direction in stroke survivors than in control subjects. Specifically, the ratios $r_2 = 16.23 \pm 3.11$ and $r_3 = 11.37 \pm 1.49$ were significantly higher in the stroke group than in the control group ($r_2 = 4.26 \pm 0.48$ and $r_3 = 3.76 \pm 0.44$, $P< 0.01$), indicating greater unintended coupling from distal to proximal joints in stroke survivors..

Abnormal synergy patterns

The systematic procedure revealed distinct abnormal synergy patterns for intended shoulder, elbow, and wrist movements in the stroke group (Fig. 3). Our novel approach delineated nine synergy patterns, including eight abnormal patterns represented by fan-shaped areas and one normal pattern at the center (circle). The control group consistently showed minimal coupling at unintended joints, with data points clustering in the central circle. In contrast, the stroke group exhibited significant inter-joint coupling, with data points widely scattered into the eight fan-shaped areas (shaded in Fig. 3).

For shoulder movements, one abnormal synergy pattern appeared in the left area, indicating coupled elbow flexion torque (Left column, Fig. 3). For elbow movements, two abnormal patterns were observed in the left and right areas, reflecting deficits in motor coordination with coupled shoulder horizontal adduction or abduction torques, respectively (Middle column, Fig. 3). For wrist movements, four abnormal synergy patterns emerged, with two prominent patterns: 1) coupled shoulder horizontal adduction and elbow flexion torques (bottom-left area), and 2) coupled shoulder horizontal abduction and elbow extension torques (top-right area) (Right column, Fig. 3). Minor patterns included 1) coupled shoulder horizontal adduction and elbow extension torques (top-left area) and 2) coupled shoulder horizontal abduction and elbow flexion torques (bottom-right area) (Right column, Fig. 3). These findings highlight distinctive motor coordination profiles in stroke survivors, characterized by specific abnormal synergy patterns during constrained upper limb tasks.

Correlations with clinical scales

Stroke survivors were each evaluated for spasticity, muscle strength and UE function using MAS and FMA. Table 2 shows point biserial correlation coefficients between elements of X_φ&X_τ, and clinical scales. The proximal score (i.e., shoulder and elbow (SE)) and the distal score (i.e., wrist and hand (WH)) were for FMA. Muscle spasticity on elbow (MAS(E)) and wrist (MAS(W)) were also involved in correlation analysis. Interestingly, we found a significant negative correlation between the LOI values, when the elbow and wrist joints were non-instructed, and spasticity, indicating that participants with higher spasticity exhibited greater inter-joint coupling deficits.

Performance of individual joint movement

Range of motion (ROM) and range of torque (ROT) at instructed joints in the unconstrained and constrained conditions, respectively, are shown in Figures 4a and 4b. Under the unconstrained condition, the stroke group had smaller ROM at all joints compared to controls, with the difference increasing from shoulder to wrist. Repeated measures ANOVA

Author Manuscript Author Manuscript Author Manuscript Author Manuscript

showed a significant Group × Joint interaction ($F_{2,124}$=22.997, P<0.001), and pairwise comparisons confirmed significantly lower ROM in the stroke group at all joints (SHL: p=0.018, ELB: P<0.001, and WRS: P<0.001). For ROT in the constrained condition, the stroke group had lower ROT at the elbow joint as compared to the control group. The ANOVA revealed a significant interaction effect Group × Joint ($F_{2,124}$=10.208, P<0.001), and pairwise comparisons revealed that ROT at elbow joint in the stroke group was significantly smaller as compared to the control group (P=0.005) while ROT at other joints did not differ between groups (SHL: P=0.521 and WRS: P=0.056). In addition, there was no significant effect on movement directions, showing that both ROM and ROT remained unchanged between inward and outward movements.

Movement rates during inward and outward movements (Figs. 4c, 4d) were significantly slower in the stroke group for all joints in both conditions, with the difference increasing from shoulder to wrist. Repeated measures ANOVA revealed a significant Group × Joint interaction in both unconstrained ($F_{2,124}$=20.877, P<0.001) and in the constrained condition ($F_{2,124}$=23.583, P<0.0001). Pairwise comparisons confirmed significantly slower rates at elbow and wrist in the stroke group in the unconstrained condition (Inward: SHL: P=0.163, ELB: P=0.02, and WRS: P<0.001; Outward: SHL: P=0.15, ELB: P=0.02, and WRS: P=0.001). and at all joints in the constrained condition (Inward: SHL: P=0.003, ELB: P<0.001, and WRS: P<0.001; Outward: SHL: P=0.011, ELB: P=0.001, and WRS: P<0.001).

SPARC, reflecting movement smoothness (Figs. 4e, 4f), was significantly lower in the stroke group at the elbow and wrist in both conditions, with values decreasing from proximal to distal joints. Repeated measures ANOVA showed significant Group × Joint interactions in both unconstrained ($F_{2,130}$=6.013, P=0.003) and in the constrained condition ($F_{2,130}$=30.163, P=0.006). Pairwise comparisons confirmed lower SPARC in the stroke group at the elbow and wrist (Unconstrained: SHL: P=0.13, ELB: p=0.012, and WRS: P=0.006; Constrained: SHL: P=0.135, ELB: P=0.042, and WRS: P=0.014) with no significant differences at the shoulder.

Discussion

This study examined the loss of joint movement individuation in the upper extremity (UE) after stroke. Using our novel approach, which identifies nine synergy patterns (one normal and eight abnormal), we detected abnormal synergies in stroke survivors. LOI was quantified as torque or angular movement at non-instructed joints normalized by instructed joint movement. Both kinematic and kinetic LOI were significantly lower in the stroke group than in controls, indicating motor deficits in joint isolation. Abnormal LOI was particularly pronounced in distal joints that should have remained fixed during instructed joint movement. Notably, the stroke group showed greater difficulty exerting individuated torque at the wrist, with motor deficits worsening distally. Previous studies found that distal-focused robotic treatment yielded greater UE function improvements than proximal-focused treatment[15,36]. This may be due to distal-focused interventions enhancing motor function at both distal and proximal joints. Combined with prior findings, our results suggest that improving distal joint individuation enhances overall UE motor function[37,38] , aligning with our observation that distal joint isolation deficits are more severe than proximal ones.

Author Manuscript Author Manuscript Author Manuscript Author Manuscript

Our analysis revealed that stroke survivors exhibited pronounced LOI, especially in the distal wrist joint, reflecting more severe motor deficits distally. This distal predominance may stem from a combination of altered neural control and biomechanical properties. The corticospinal tract (CST), which plays a critical role in controlling fine distal limb movements, is often compromised after stroke, leading to impaired joint individuation[7]. In contrast, the reticulospinal tract (RST), which primarily influences proximal and axial muscles, may become upregulated to compensate for CST deficits[8]. As a result, attempts to move distal joints like the wrist may inadvertently activate the RST, leading to unintended movements in proximal joints such as the shoulder. While neural mechanisms are likely the primary drivers of these abnormal movement patterns, biomechanical factors may further amplify them. Specifically, proximal joints like the shoulder possess greater muscle mass and generate higher torques than distal joints, making them more susceptible to producing unintended motion when broadly recruited through RST pathways.

These mechanical and neural factors together contribute to the significant increase in the $\|X_{\tau a}\|/\|X_{\tau s}\|$) asymmetry measure observed in stroke survivors compared to controls, indicating more asymmetric torque coupling. Notably, distal-to-proximal joint coupling was significantly higher than the opposite direction, reflecting less coordinated joint interactions and greater distal joint impairments. This asymmetry highlights disrupted motor coordination and irregularities in multi-joint coupling after stroke. Furthermore, the ratios r_2 and r_3, representing distal-to-proximal coupling effects, were significantly higher in the stroke group, indicating increased unintended proximal torque (shoulder and elbow) during distal joint (wrist) movements. This suggests impaired motor control and reduced joint independence, characteristic of stroke-related deficits. Interestingly, the ratio r_1, reflecting coupling between shoulder and elbow joints, did not differ significantly between groups. This implies stroke selectively affects coupling, with more pronounced disruptions during distal joint movements. These findings, coupled with correlations between LOI and clinical scales (FMA and MAS), suggest that individuals with poorer motor function and higher spasticity levels demonstrate more pronounced abnormal coupling and reduced joint individuation. This relationship highlights the clinical relevance of LOI measures, providing insight into how biomechanical deficits correspond with functional impairments.

Weight support used in our experimental setup may have further influenced these coupling patterns. This study involved horizontal plane motions with arm weight support, under which the observed gradient showed reduced proximal coupling at the shoulder and elbow. This may explain the discrepancies between our findings and those of the two previous studies,[9,10] both of which employed unsupported 3D reaching tasks and reported stronger proximal synergies. Without weight support, the coupling at proximal joints during distal movements may become more pronounced, highlighting how task conditions influence coupling and synergy expression. In contrast, the wrist's reliance on CST input means it benefits less from weight support, which may explain the more pronounced synergy expression and increased reliance on RST control observed in distal joints.

Importantly, spasticity has also been involved in this maladaptive reorganization. Increased reliance on the RST following CST damage may heighten synergy severity and exacerbate spasticity, particularly in upper limb flexors. Spasticity and abnormal synergies share

Author Manuscript Author Manuscript Author Manuscript Author Manuscript

common neural substrates within the RST, known for its broad, non-specific activation patterns, which may explain the co-occurrence of increased muscle tone and loss of independent joint control post-stroke. Rehabilitation strategies targeting distal joint individuation, such as distal-focused robotic therapy, have shown promise in improving both distal and proximal functions by mitigating RST overactivity and promoting neuroplastic changes. These findings underscore the importance of incorporating therapies that emphasize distal joint control to optimize motor recovery and reduce the dual burden of spasticity and impaired coordination in stroke rehabilitation.

The ability to control and isolate UE movement at specific joints is essential for many human behaviors. Few studies have directly examined individuation of joint movements. Hager-Ross and Schieber (2000)[42] showed that when healthy subjects attempt to move a single finger, there is often some motion at adjacent fingers. Movements of the thumb, index finger and little finger typically were more highly individuated than were movements of the middle or ring fingers. Even though the differences may be due to the way the musculature is constructed, particularly the organization of multi-tendon finger muscles, long-term motor experiences and variations in the central inputs to spinal motoneuron pools play significant roles in these differences[42]. Studies of arm control have tested motions similar to our individuated movements[43,44]. They find that the non-moving joints are actively stabilized in a predictive manner throughout movement of a single joint. Stabilization is necessary in an individuated movement to offset the forces induced by biarticular muscles and/or to offset the rotational forces that arise due to the motions of linked joints (interaction torques). In this sense, joint individuation is a more global measure of reaching performance relative to measures such as strength, sensation or spasticity. However, the interplay between joint individuation and spasticity should not be overlooked, as increased spastic tone may further limit an individual's ability to stabilize adjacent joints during isolated movements, thereby compounding the difficulty of achieving precise motor control. The ability to individuate reflects specific motor control problems essential to reaching movement.

The control group demonstrated strong individuation of all upper extremity (UE) joint movements, excelling at the wrist and performing progressively worse at the elbow. Wrist individuation likely benefited from the smaller hand mass, requiring minimal stabilization of proximal joints and producing low interaction torques[45]. Additionally, crossed pathways for distal musculature and ipsilateral pathways for proximal musculature may contribute to these differences. However, we did not monitor whether the non-tested arm remained silent, which might have influenced individuation, particularly at proximal joints.

The cross-sectional area and moment arms of wrist muscles are small, limiting their influence on elbow movement[46]. While wrist motions may have induced finger movement, finger motion was not evaluated in this study. The elbow was the most difficult joint to individuate, potentially due to the involvement of biarticular muscles, unlike the shoulder, which can theoretically be controlled by monoarticular muscles. However, both joints require stabilization of non-moving joints to offset interaction torques [43,47] . Another explanation could be related to motor experiences, as daily activities often involve moving the shoulder while stabilizing other joints, whereas such stabilization during elbow movements is less common.

Author Manuscript Author Manuscript Author Manuscript Author Manuscript

Stroke survivors struggled to individuate all joint movements, typically producing unwanted flexion at the shoulder and elbow, sometimes more at non-instructed joints than instructed ones. Notably, contrary to the expectation that isolated flexion would present more challenges than extension, our findings revealed similar levels of impairment during both inward (flexion) and outward (extension) movements. This suggests that extensor synergy was as prevalent as flexor synergy among stroke survivors, a finding that warrants attention as extensor synergies have been less explored in previous literature. The comparable levels of impairment may reflect symmetrical involvement of descending motor pathways or compensatory neural reorganization affecting both flexors and extensors post-stroke. This observation underscores the need to consider both synergy types in rehabilitation strategies aimed at improving joint individuation.

Although not evaluated, concurrent wrist and finger motion may have been more common in hemiparetic subjects than controls. Moreover, we did not assess whether hemiparetic subjects produced the correct instructed movement, an important area for future research. Future studies should also explore how varying levels of spasticity influence individuation at different joints, particularly given the potential for spastic hypertonia to disproportionately affect distal movements through enhanced RST involvement. Additionally, variations in stroke severity within the stroke cohort and the age difference between the stroke and control groups are potential limitations. However, controlling for these factors in stroke studies is inherently challenging, especially considering the wide variability in stroke presentations and substantial age variability within each group. The simplicity of the task likely minimized the impact of age differences on performance between groups. This study's limitations include the use of a gravity-supported exoskeleton, which might have influenced the observed joint coupling patterns. While our setup facilitated the analysis within a horizontal plane with arm weight support, it may not fully represent the natural conditions of daily activities. Consequently, our findings regarding joint coupling and synergy should be cautiously interpreted, considering the potential alteration of motor control strategies in an unsupported environment. Future studies should aim to replicate these findings in more functionally relevant settings to enhance the generalizability of our conclusions.

In conclusion, we investigated UE individuation post-stroke using a novel approach to identify 2–3 abnormal synergy patterns among nine possible movement synergies. Stroke survivors exhibited significantly higher torques and angles at non-instructed joints compared to controls, with increased coupling at proximal joints during distal joint movements. These findings reveal a proximal-to-distal gradient in motor control deficits and highlight the presence of abnormal synergy patterns associated with stroke-related motor impairment[48]. Additionally, considering the influence of spasticity and its neural underpinnings in the RST may further refine rehabilitation strategies, enabling more comprehensive approaches to mitigate both synergy-related and spastic motor impairments post-stroke.

Funding

This research was supported in part by the National Institute on Disability, Independent Living, and Rehabilitation Research (NIDILRR 90DP0099, 90REMM0001) and the NIH (P30 AG028747).

Author Manuscript Author Manuscript Author Manuscript Author Manuscript

Data availability

The datasets generated during and/or analyzed during the current study are available from the corresponding author on reasonable request.

References

1. Virani SS, Alonso A, Aparicio HJ, et al. Heart Disease and Stroke Statistics-2021 Update: A Report From the American Heart Association. Circulation. Feb 23 2021;143(8):e254–e743. doi:10.1161/CIR.0000000000000950 [PubMed: 33501848]
2. Johnson W, Onuma O, Owolabi M, Sachdev SJBotWHO. Stroke: a global response is needed. 2016;94(9):634.
3. Lee KB, Lim SH, Kim KH, et al. Six-month functional recovery of stroke patients: a multi-time-point study. Int J Rehabil Res. Jun 2015;38(2):173–80. doi:10.1097/MRR.0000000000000108 [PubMed: 25603539]
4. Langhorne P, Bernhardt J, Kwakkel G. Stroke rehabilitation. Lancet. May 14 2011;377(9778):1693–702. doi:10.1016/S0140-6736(11)60325-5 [PubMed: 21571152]
5. Kwakkel G, Kollen BJ, Wagenaar RC. Therapy impact on functional recovery in stroke rehabilitation: a critical review of the literature. Physiotherapy. 1999;85(7):377–391.
6. Twitchell TE. The restoration of motor function following hemiplegia in man. Brain. Dec 1951;74(4):443–80. doi:10.1093/brain/74.4.443 [PubMed: 14895765]
7. Beer RF, Dewald JP, Rymer WZ. Deficits in the coordination of multijoint arm movements in patients with hemiparesis: evidence for disturbed control of limb dynamics. Exp Brain Res. Apr 2000;131(3):305–19. doi:10.1007/s002219900275 [PubMed: 10789946]
8. Levin MF. Interjoint coordination during pointing movements is disrupted in spastic hemiparesis. Brain. Feb 1996;119 (Pt 1):281–93. doi:10.1093/brain/119.1.281 [PubMed: 8624689]
9. Lang CE, Schieber MH. Differential impairment of individuated finger movements in humans after damage to the motor cortex or the corticospinal tract. J Neurophysiol. Aug 2003;90(2):1160–70. doi:10.1152/jn.00130.2003 [PubMed: 12660350]
10. Wolbrecht ET, Rowe JB, Chan V, Ingemanson ML, Cramer SC, Reinkensmeyer DJ. Finger strength, individuation, and their interaction: Relationship to hand function and corticospinal tract injury after stroke. Clinical Neurophysiology. 2018;129(4):797–808. [PubMed: 29453171]
11. Zackowski KM, Dromerick A, Sahrmann S, Thach W, Bastian AJB. How do strength, sensation, spasticity and joint individuation relate to the reaching deficits of people with chronic hemiparesis? 2004;127(5):1035–1046.
12. Beer RF, Given JD, Dewald JP, rehabilitation. Task-dependent weakness at the elbow in patients with hemiparesis. Archives of physical medicine. 1999;80(7):766–772.
13. Dewald JP, Beer RF. Abnormal joint torque patterns in the paretic upper limb of subjects with hemiparesis. Muscle Nerve. Feb 2001;24(2):273–83. doi:10.1002/1097-4598(200102)24:2<273::aid-mus130>3.0.co;2-z [PubMed: 11180211]
14. Ellis MD, Acosta AM, Yao J, Dewald JP. Position-dependent torque coupling and associated muscle activation in the hemiparetic upper extremity. Exp Brain Res. Feb 2007;176(4):594–602. doi:10.1007/s00221-006-0637-x [PubMed: 16924488]
15. Dipietro L, Krebs HI, Fasoli SE, Volpe BT, Hogan N. Submovement changes characterize generalization of motor recovery after stroke. Cortex. 2009;45(3):318–324. [PubMed: 18640668]
16. Fugl-Meyer AR, Jaasko L, Leyman I, Olsson S, Steglind S. The post-stroke hemiplegic patient. 1. a method for evaluation of physical performance. Scand J Rehabil Med. 1975;7(1):13–31. [PubMed: 1135616]
17. Ren Y, Kang SH, Park H-S, Wu Y-N, Zhang L-Q. Developing a Multi-Joint Upper Limb Exoskeleton Robot for Diagnosis, Therapy, and Outcome Evaluation in Neurorehabilitation. IEEE Trans Neural Systems Rehab Eng. 2013;21(3):490–499. doi:10.1109/TNSRE.2012.2225073

Author Manuscript Author Manuscript Author Manuscript Author Manuscript

18. Housman SJ, Scott KM, Reinkensmeyer DJ. A randomized controlled trial of gravity-supported, computer-enhanced arm exercise for individuals with severe hemiparesis. Neurorehabil Neural Repair. Jun 2009;23(5):505–14. doi:10.1177/1545968308331148 [PubMed: 19237734]
19. Cirstea MC, Levin MF. Compensatory strategies for reaching in stroke. Brain. May 2000;123 (Pt 5):940–53. doi:10.1093/brain/123.5.940 [PubMed: 10775539]
20. Baker SN. The primate reticulospinal tract, hand function and functional recovery. J Physiol. Dec 1 2011;589(Pt 23):5603–12. doi:10.1113/jphysiol.2011.215160 [PubMed: 21878519]
21. Lemon RN. Descending pathways in motor control. Annu Rev Neurosci. 2008;31:195–218. doi:10.1146/annurev.neuro.31.060407.125547 [PubMed: 18558853]
22. Zaaimi B, Dean LR, Baker SN. Different contributions of primary motor cortex, reticular formation, and spinal cord to fractionated muscle activation. J Neurophysiol. Jan 1 2018;119(1):235–250. doi:10.1152/jn.00672.2017 [PubMed: 29046427]
23. Schieber MH. Constraints on somatotopic organization in the primary motor cortex. J Neurophysiol. Nov 2001;86(5):2125–43. doi:10.1152/jn.2001.86.5.2125 [PubMed: 11698506]
24. Lang CE, Schieber MH. Human finger independence: limitations due to passive mechanical coupling versus active neuromuscular control. J Neurophysiol. Nov 2004;92(5):2802–10. doi:10.1152/jn.00480.2004 [PubMed: 15212429]
25. Krebs HI, Volpe BT, Williams D, et al. Robot-aided neurorehabilitation: a robot for wrist rehabilitation. IEEE Trans Neural Syst Rehabil Eng. Sep 2007;15(3):327–35. doi:10.1109/TNSRE.2007.903899 [PubMed: 17894265]
26. Hu XL, Tong RK, Ho NS, Xue JJ, Rong W, Li LS. Wrist Rehabilitation Assisted by an Electromyography-Driven Neuromuscular Electrical Stimulation Robot After Stroke. Neurorehabil Neural Repair. Sep 2015;29(8):767–76. doi:10.1177/1545968314565510 [PubMed: 25549656]
27. Nam C, Rong W, Li W, Xie Y, Hu X, Zheng Y. The Effects of Upper-Limb Training Assisted with an Electromyography-Driven Neuromuscular Electrical Stimulation Robotic Hand on Chronic Stroke. Front Neurol. 2017;8:679. doi:10.3389/fneur.2017.00679 [PubMed: 29312116]
28. Zhang L-Q, Park H-S, Ren Y. Shoulder, Elbow and Wrist Stiffness in Passive Movement and Their Independent Control in Voluntary Movement Post Stroke. presented at: IEEE 11th Int Conf on Rehabilitation Robotics; June 23-26 2009; Kyoto, Japan.
29. Gladstone DJ, Danells CJ, Black SE. The fugl-meyer assessment of motor recovery after stroke: a critical review of its measurement properties. Neurorehabil Neural Repair. Sep 2002;16(3):232–40. doi:10.1177/154596802401105171 [PubMed: 12234086]
30. Page SJ, Levine P, Hade E. Psychometric properties and administration of the wrist/hand subscales of the Fugl-Meyer Assessment in minimally impaired upper extremity hemiparesis in stroke. Arch Phys Med Rehabil. Dec 2012;93(12):2373–6 e5. doi:10.1016/j.apmr.2012.06.017 [PubMed: 22759831]
31. Hsieh CL, Hsueh IP, Chiang FM, Lin PH. Inter-rater reliability and validity of the action research arm test in stroke patients. Age Ageing. Mar 1998;27(2):107–13. doi:10.1093/ageing/27.2.107
32. Pandyan AD, Johnson GR, Price CI, Curless RH, Barnes MP, Rodgers HJCr. A review of the properties and limitations of the Ashworth and modified Ashworth Scales as measures of spasticity. 1999;13(5):373–383.
33. Ansari NN, Naghdi S, Arab TK, Jalaie SJN. The interrater and intrarater reliability of the Modified Ashworth Scale in the assessment of muscle spasticity: limb and muscle group effect. 2008;23(3):231–237.
34. Beck Y, Herman T, Brozgol M, et al. SPARC: a new approach to quantifying gait smoothness in patients with Parkinson's disease. 2018;15(1):1–9.
35. Zhang LQ, Son J, Park HS, Kang SH, Lee Y, Ren Y. Changes of Shoulder, Elbow, and Wrist Stiffness Matrix Post Stroke. IEEE Trans Neural Syst Rehabil Eng. Jul 2017;25(7):844–851. doi:10.1109/TNSRE.2017.2707238 [PubMed: 28541901]
36. Mazzoleni S, Sale P, Franceschini M, et al. Effects of proximal and distal robot-assisted upper limb rehabilitation on chronic stroke recovery. NeuroRehabilitation. 2013;33(1):33–9. doi:10.3233/NRE-130925 [PubMed: 23949024]

Author Manuscript Author Manuscript Author Manuscript Author Manuscript

37. Shin J-H, Kim M-Y, Lee J-Y, et al. Effects of virtual reality-based rehabilitation on distal upper extremity function and health-related quality of life: a single-blinded, randomized controlled trial. Journal of neuroengineering rehabilitation. 2016;13:1–10. [PubMed: 26728632]
38. Zhao M, Wang G, Wang A, Cheng LJ, Lau Y. Robot-assisted distal training improves upper limb dexterity and function after stroke: a systematic review and meta-regression. Neurological Sciences. 2022;43(3):1641–1657. [PubMed: 35089447]
39. Zaaimi B, Edgley SA, Soteropoulos DS, Baker SN. Changes in descending motor pathway connectivity after corticospinal tract lesion in macaque monkey. Brain. Jul 2012;135(Pt 7):2277–89. doi:10.1093/brain/aws115 [PubMed: 22581799]
40. Mooney RA, Anaya MA, Stilling JM, Celnik PA. Heightened Reticulospinal Excitability after Severe Corticospinal Damage in Chronic Stroke. Ann Neurol. Oct 10 2024;doi:10.1002/ana.27103
41. Avni I, Arac A, Binyamin-Netser R, Kramer S, Krakauer JW, Shmuelof L. The Kinematics of 3D Arm Movements in Sub-Acute Stroke: Impaired Inter-Joint Coordination is Attributable to Both Weakness and Flexor Synergy Intrusion. Neurorehabil Neural Repair. Sep 2024;38(9):646–658. doi:10.1177/15459683241268535 [PubMed: 39113590]
42. Hager-Ross C, Schieber MH. Quantifying the independence of human finger movements: comparisons of digits, hands, and movement frequencies. J Neurosci. Nov 15 2000;20(22):8542–50. doi:10.1523/JNEUROSCI.20-22-08542.2000 [PubMed: 11069962]
43. Almeida GL, Hong DA, Corcos D, Gottlieb GL. Organizing principles for voluntary movement: extending single-joint rules. J Neurophysiol. Oct 1995;74(4):1374–81. doi:10.1152/jn.1995.74.4.1374 [PubMed: 8989378]
44. Gribble PL, Ostry DJ. Compensation for interaction torques during single- and multijoint limb movement. J Neurophysiol. Nov 1999;82(5):2310–26. doi:10.1152/jn.1999.82.5.2310 [PubMed: 10561408]
45. Virji-Babul N, Cooke JD. Influence of joint interactional effects on the coordination of planar two-joint arm movements. Exp Brain Res. 1995;103(3):451–9. doi:10.1007/BF00241504 [PubMed: 7789451]
46. Loren GJ, Shoemaker SD, Burkholder TJ, Jacobson MD, Friden J, Lieber RL. Human wrist motors: biomechanical design and application to tendon transfers. J Biomech. Mar 1996;29(3):331–42. doi:10.1016/0021-9290(95)00055-0 [PubMed: 8850639]
47. Bastian A, Zackowski K, Thach W. Cerebellar ataxia: torque deficiency or torque mismatch between joints. Journal of neurophysiology. 2000;83(5):3019–3030. [PubMed: 10805697]
48. Cheung VC, Turolla A, Agostini M, et al. Muscle synergy patterns as physiological markers of motor cortical damage. Proceedings of the national academy of sciences. 2012;109(36):14652–14656.

Author Manuscript Author Manuscript Author Manuscript Author Manuscript

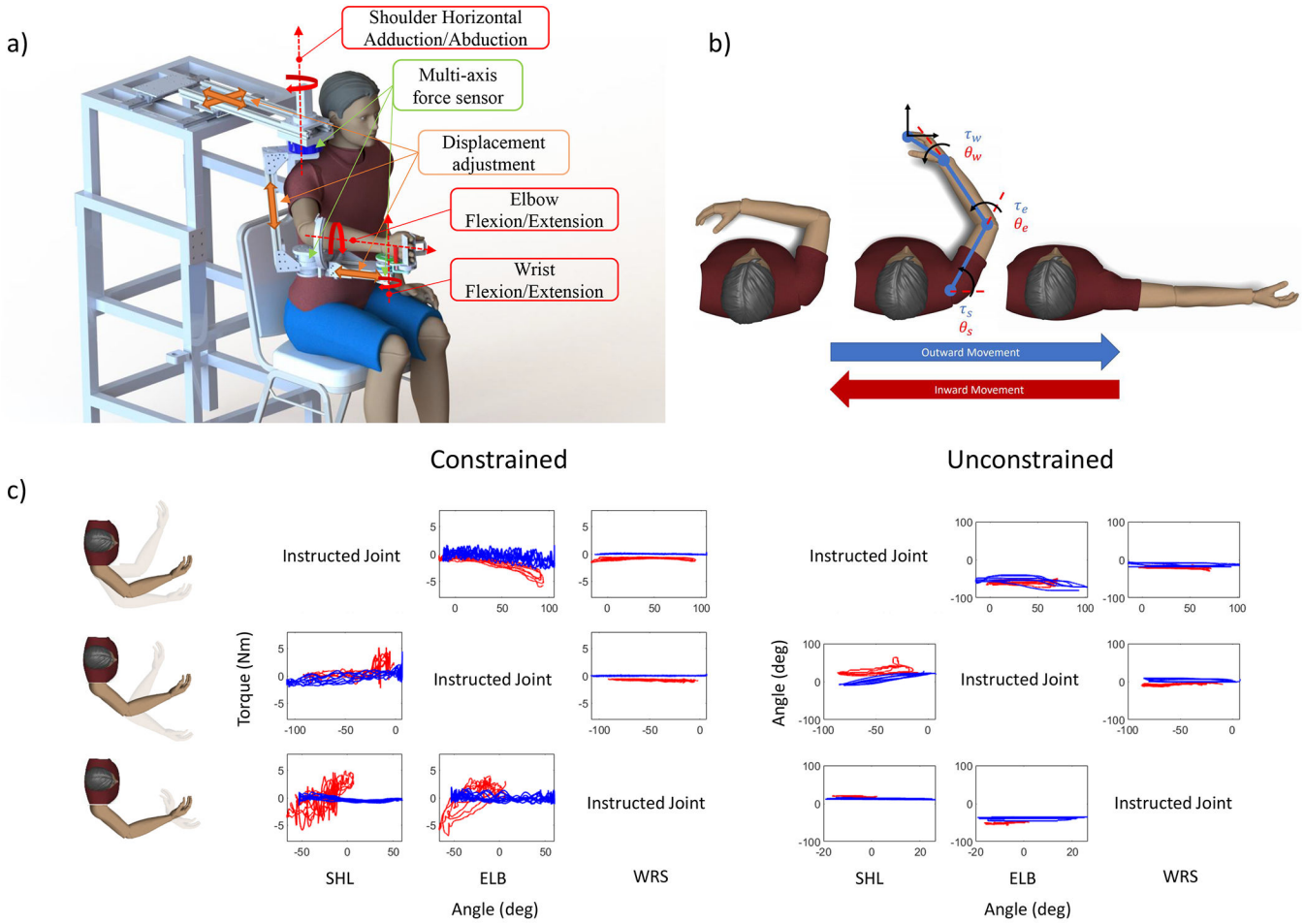


Figure 1.

(a) A multi-joint rehabilitation robot, called IntelliArm, controls the shoulder, elbow, and wrist movement simultaneously. The shoulder horizontal abduction/adduction, and elbow and wrist flexion/extension are controlled by the shoulder, elbow, and wrist motors of the IntelliArm, respectively. Each segment length of the IntelliArm was adjusted to match the participants' segment length. The subject was seated with the upper arm, forearm and hand strapped to the IntelliArm. (b) top view of the horizontal plane. (c) During an instructed joint movement, angles and torques at all three joints were measured in outward and inward direction, with the left and right 3x3 grid of subplots showed the non-instructed joint under constrained condition and unconstrained condition, respectively, for a representative control subject (blue) and stroke survivor (red).

Author Manuscript Author Manuscript Author Manuscript Author Manuscript

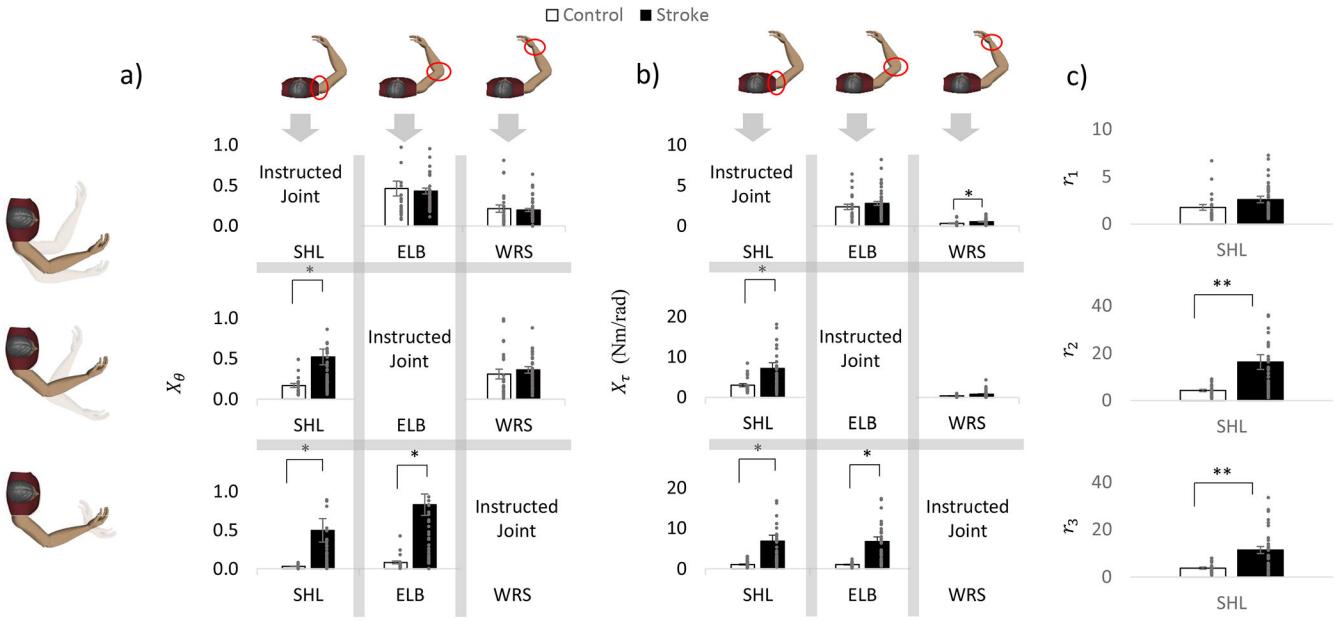


Figure 2.

LOI between the control group (open bar) and stroke group (closed bar) in the unconstrained condition (X_θ in a)) and in the constrained condition (X_τ in b)). The first, second and third rows correspond to a shoulder, elbow and wrist movement tasks, respectively. Red circles indicate the joints where measurements were taken. The first, second and third columns correspond to the LOI index at the shoulder, elbow, and wrist, respectively. The LOI indicates the degree of difficulty in controlling individual joints independently, with higher LOI indicating greater difficulty. The LOI differences between the groups increased from proximal to distal joints. In c), the ratios $r_1 = X_{\tau 21}/X_{\tau 12}$, $r_2 = X_{\tau 31}/X_{\tau 13}$ and $r_3 = X_{\tau 32}/X_{\tau 23}$ are included to further highlight these group differences. Gray dots represent individual data points for each group. Significant differences between groups revealed by pairwise comparisons were indicated with the asterisk (*<0.05, **<0.001). Error bars represent SEM across subjects.

Author Manuscript Author Manuscript Author Manuscript Author Manuscript

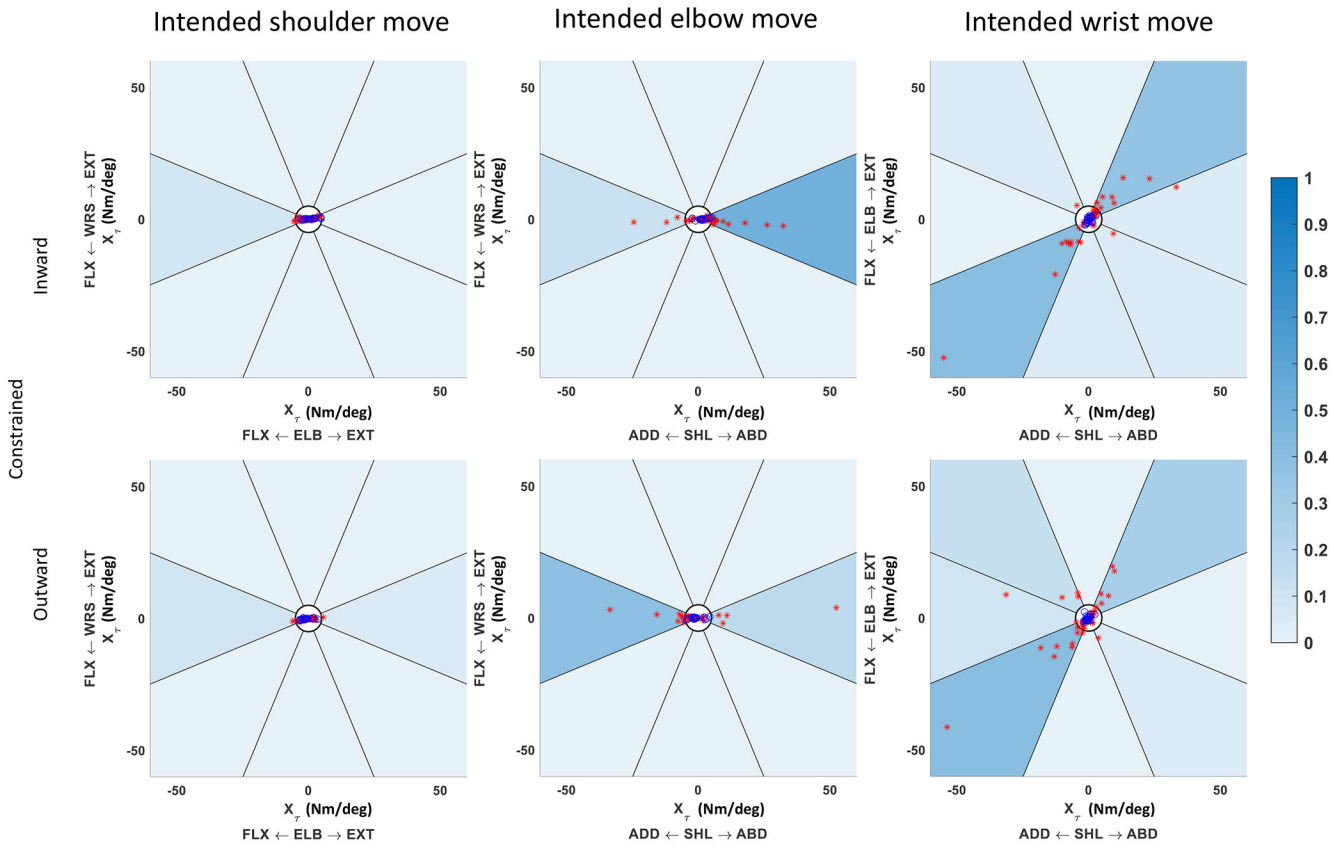


Figure 3.

Abnormal synergy patterns identified from a total nine synergy patterns during individual joint motor tasks under constrained conditions. For each individual joint motor task, there are 9 possible synergy patterns depicted by a circle at the center and eight 45-degree fan-shaped areas. The color bar on the right shows the proportion of subjects with abnormal patterns in each area, ranging from 0 to 1. The darker shaded areas indicate where more subjects showed abnormal synergy patterns. Individual subject's LOI data for the control and stroke groups are shown in blue circles and red asterisks, respectively.

Author Manuscript Author Manuscript Author Manuscript Author Manuscript

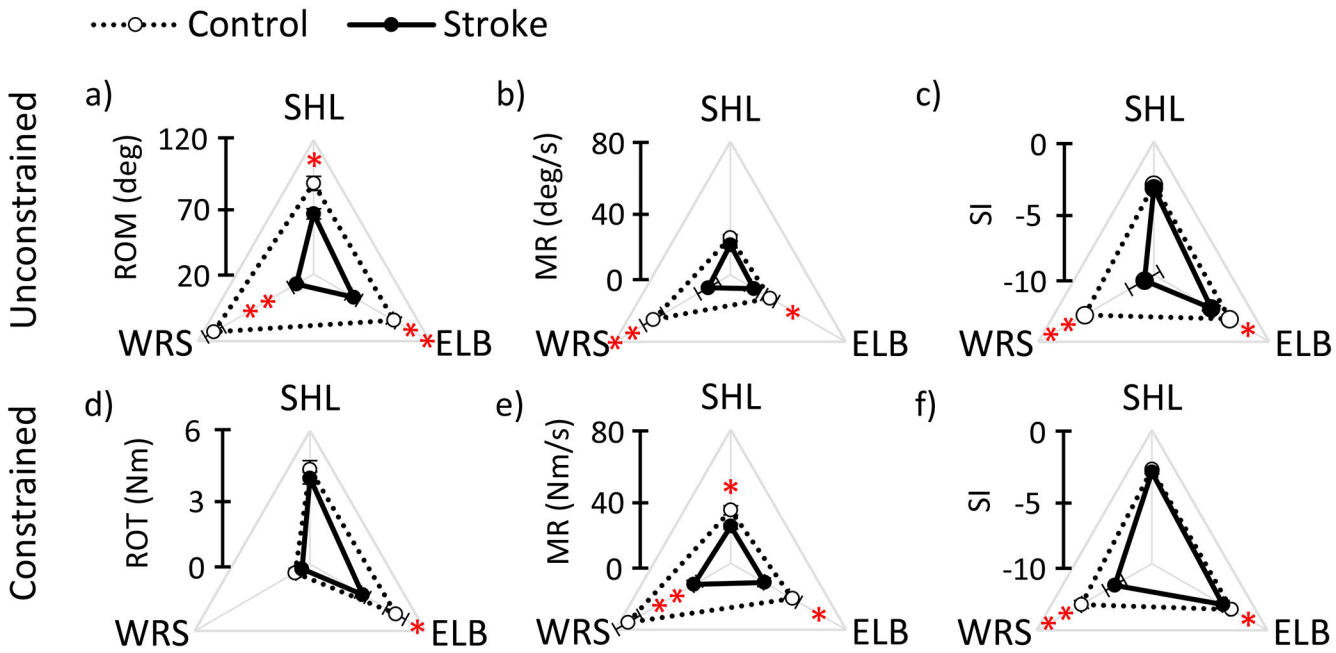


Figure 4.

a) Range of motion (ROM), b) movement rate (MR), and c) smoothness index (SI) in the unconstrained condition; d) range of torque (ROT), e) movement rate (MR), and f) smoothness index (SI) in the constrained condition. A significant interaction effect between Group and Joint was found for all variables (ROM, ROT, MR, and SI), with significant differences between groups indicated by asterisks (*$p < 0.05$, **$p < 0.001$). An asterisk was added for the shoulder direction in the unconstrained condition for movement rate to reflect the statistical findings. Error bars represent SEM across subjects.

Author Manuscript

Author Manuscript

Author Manuscript

Author Manuscript

Table1.

Demographic and clinical characteristics of stroke survivors

	Characteristic		N = 53
Demographics	Age, Mean ± SD (years)		58 (±13.1)
	Gender	Male, n (%)	34 (64%)
		Female, n (%)	19 (36%)
Stroke-Specific Details	Stroke Type	Ischemic, n (%)	41 (77%)
		Hemorrhagic, n (%)	12 (23%)
	Side Affected	Left, n (%)	27 (51%)
		Right, n (%)	26 (49%)
	Time Since Stroke, Mean ± SD (months)		14.2 (±8.7)
Clinical Assessment Scores	Modified Ashworth Scale	Elbow, Mean ± SD	1.8 (±0.9)
		Wrist, Mean ± SD	1.5 (±0.8)
	Fugl-Meyer Assessment	Total Score, Mean ± SD	42.5 (±10.2)
		Proximal, Mean ± SD	23.4 (±5.1)
		Distal, Mean ± SD	19.1 (±6.3)

Author Manuscript Author Manuscript Author Manuscript Author Manuscript

Table 2.

Spearman correlation coefficients among clinical assessments, and X_θ and X_τ elements

	SHL		ELB		WRS	
	$X_{\tau 12}$	$X_{\tau 13}$	$X_{\tau 21}$	$X_{\tau 23}$	$X_{\tau 31}$	$X_{\tau 32}$
MAS (E)	0.081	0.134	**0.464** **	**0.450** **	0.214	**0.339** *
MAS (W)	0.084	0.075	**0.333** *	**0.336** *	0.232	**0.322** *
FMA	−0.066	−0.006	**−0.429** **	**−0.359** *	**−0.400** **	**−0.426** **
FMA (SE)	0.088	0.129	**−0.463** **	**−0.392** *	**−0.473** **	**−0.472** **
FMA (WH)	0.164	0.146	−0.312	−0.194	−0.319	**−0.367** *
	$X_{\theta 12}$	$X_{\theta 13}$	$X_{\theta 21}$	$X_{\theta 23}$	$X_{\theta 31}$	$X_{\theta 32}$
MAS (E)	−0.260	−0.044	**−0.423** *	−0.030	**0.335** *	**0.423** **
MAS (W)	0.070	−0.189	0.282	−0.140	0.287	**0.379** *
FMA	0.146	0.061	**−0.394** **	0.144	**−0.390** *	**−0.442** **
FMA (SE)	0.212	0.011	**−0.455** **	0.162	**−0.427** *	**−0.405** *
FMA (WH)	0.106	0.037	**−0.384** *	0.174	**−0.377** *	**−0.488** **

MAS: Modified Ashworth Scale, E: elbow, W: Wrist; FMA: Fugl-Meyer Assessment, SE, shoulder and elbow; WH, wrist and hand.

* $P < 0.05$,

** $P < 0.01$.